VIP Chalcogenides Very Important Paper

How to cite: *Angew. Chem. Int. Ed.* **2021**, *60*, 22570–22577
International Edition: doi.org/10.1002/anie.202107642
German Edition: doi.org/10.1002/ange.202107642

Chalcogenides by Reduction of their Dioxides in Ultra-Alkaline Media

*Ralf Albrecht and Michael Ruck**

Abstract: *The reaction of chalcogen dioxides ChO_2 (Ch = Se, Te) with As_2O_3 in a 30 molar KOH hydroflux at about 200 °C yielded crystals of potassium trichalcogenides K_2Ch_3 with dimensions up to 2 cm. Arsenic trioxide acts as electron donor and is oxidized to arsenate(V). The new heterochalcogenide anion $(TeSe_2)^{2-}$ formed when starting from SeO_2 and TeO_2 simultaneously. The compound K_2TeSe_2 crystallizes isostructural to K_2S_3 and K_2Se_3. The unexpected redox reaction as well as the precipitation of hygroscopic compounds from an aqueous solution are attributed to a strongly reduced activity of water. The reactions were studied by Raman and UV/Vis spectroscopy. Depending on the concentration of As_2O_3, colorless monochalcogenide Ch^{2-} or orange Se_2^{2-} and purple Te_2^{2-} anions are dominating the solutions.*

Introduction

The history of alkali metal selenides and tellurides reaches back at least to the beginning of the last century, when the groups of *Zintl* and *Klemm* obtained such compounds from reactions in liquid ammonia at −78 °C.[1–3] They were able to isolate single-crystals and to determine the crystal structures of several alkali metal chalcogenides A_2Ch (A = Li—K, Ch = Se, Te), which contain closed-shell Ch^{2-} anions. Forty years later, single-crystals of the triselenide K_2Se_3 were synthesized under ammonothermal conditions (150 °C, 500 bar) in an autoclave starting from the elements.[4] Concurrently, the first tritelluride K_2Te_3 was obtained from the elements at about 600 °C in a welded iron autoclave.[5] The trichalcogenide anions Ch_3^{2-} are angulated molecules (Se_3^{2-} 102.5°; Te_3^{2-} 104.4°)[4,5] with a negative (formal) charge on each of the terminal atoms. Using similar procedures, single-crystals of several oligoselenides and tellurides were synthesized, for example, K_2Ch_2,[6] K_5Ch_3 (Ch = Se, Te)[7,8] and also the hetero-trichalcogenide K_2TeSe_3.[9] Alternatively, potassium chalcogenides, such as β-K_2Se_2 or K_2Se_4, were obtained by solvothermal synthesis in an organic solvent, for example, *N*,*N*-dimethylformamide (DMF) or ethane-1,2-diamine.[10] As the starting materials and reaction products are sensitive to oxygen and moisture, all described methods necessitate consequent handling under inert gas to exclude water.

Accordingly, we were highly surprised to obtain such sensitive compounds with reduced chalcogen species from an aqueous medium starting from chalcogen(IV) oxides. We had applied the new hydroflux method,[11] which utilizes a highly concentrated mixture of alkali metal hydroxide and water with a molar ratio $q(A) = n(H_2O):n(AOH)$ close to one (i.e. 30 to 50 molar) as reaction medium. Commonly, sodium or potassium hydroxide are employed. The hydroflux provides simple and fast synthesis of crystalline metal oxides and hydroxides in almost quantitative yield.[12,13] Typically, the hydroflux reaction is completed within 10 hours at about 200 °C in a stainless steel autoclave with a PTFE inlet, which endures the ultra-alkaline conditions and prevents the loss of water. As the activity of the water is dramatically reduced in such aqueous salt melts, the pressure evolving during the hydroflux reaction is much lower than under hydrothermal conditions. The hydroflux medium tends to promote higher oxidations states than expected for a diluted aqueous system. For example, the oxidation of arsenic(III) and chromium(III) to their maximum oxidation states was observed.[14,15]

In the following, we report studies on the reduction of SeO_2 and TeO_2 by As_2O_3 in a KOH hydroflux, resulting in crystals of K_2Se_3, K_2Te_3 and the new hetero-trichalcogenide K_2TeSe_2.

Results and Discussion

To understand the reactions in the hydroflux systems, a brief review of the chemistry of chalcogens under reductive conditions in various other media is helpful.

In liquid ammonia, solutions of tellurides adapt a characteristic color depending on the anionic species formed. When adding an alkali metal A to liquid ammonia, an intense blue color caused by solvated electrons appears immediately. The latter are able to reduce tellurium to form different tellurides: Te^{2-} anions form a white precipitate (A_2Te), Te_2^{2-} anions turn the solution deep violet-blue, and Te_3^{2-} anions have an intense wine-red color.[16] When DMF is used as solvent, no sequence of differently colored solutions occurs, as firstly the starting elements are insoluble in DMF and secondly no solvated electrons are present in the solution. When stirring elemental tellurium and an alkali metal in a DMF solution at room temperature, in the beginning no reaction is observed

[*] R. Albrecht, Prof. Dr. M. Ruck
Faculty of Chemistry and Food Chemistry, Technische Universität Dresden
01069 Dresden (Germany)
E-mail: michael.ruck@tu-dresden.de
Homepage: https://tu-dresden.de/mn/chemie/ac/ac2
Prof. Dr. M. Ruck
Max-Planck Institute for Chemical Physics of Solids
Nöthnitzer Straße 40, 01187 Dresden (Germany)
Supporting information and the ORCID identification number(s) for the author(s) of this article can be found under: https://doi.org/10.1002/anie.202107642.

visually.[17] After half an hour, the DMF solution develops a faint pink color that intensifies to deep purple over the course of hours. The tellurium and alkali metal appear to react by physical contact resulting in the formation of Te^{2-} anions, which are soluble in DMF.[18] Those monotelluride anions react with remaining tellurium metal to form oligotellurides, which are linked by the equilibrium (1):

$$Te^{2-} + Te_3^{2-} \rightleftharpoons 2\,Te_2^{2-} \quad (1)$$

When pre-synthesized alkali metal tellurides are dissolved in DMF, the same deep purple colored solutions form, independent of the *A*:Te ratio and the nature of the alkali metal *A*.[18]

In contrast to the tellurides, the chemistry of selenides in O_2-free aqueous systems was investigated in several spectroscopic and electrochemical studies.[19–23] In those experiments, dissolved H_2Se was oxidized by H_2O_2 or reacted with elemental selenium. The equilibria (2) and (3) between four species Se_n^{2-} with $n = 1$–4 in low-concentrated alkaline solutions were proposed:[20]

$$Se^{2-} + Se_3^{2-} \rightleftharpoons 2\,Se_2^{2-} \quad (2)$$

$$Se^{2-} + 2\,Se_4^{2-} \rightleftharpoons 3\,Se_3^{2-} \quad (3)$$

At room temperature and at pH 14, the product sides of both equilibria are preferred.[19,20] In the range between pH 7 and pH 5, an approximately equal concentration of diselenide Se_2^{2-} and triselenide Se_3^{2-} anions was observed.[21] The protonated selenides species HSe^- ($pK_a = 15.0$) and HSe_2^- ($pK_a = 9.3$) were observed even in 1 M KOH solutions, however, when doubling the base concentration both anions were essentially deprotonated.[19,23]

In our experiments, the syntheses of selenides and tellurides were performed under hydroflux conditions in a stainless-steel autoclave with PTFE inlet. The reaction medium consisted of a potassium hydroxide hydroflux with $q(K) = n(H_2O):n(KOH) = 1.9$ (i.e. about $30\,mol\,L^{-1}$). At room temperature this is a clear solution with a small residuum of solid KOH. The starting materials SeO_2, TeO_2, and As_2O_3 are well-soluble in highly alkaline media. The use of other reducing agents, e.g., V_2O_3, VO_2, or Sb_2O_3, is also possible, but they differ in their solubility under hydroflux conditions. For example, V_2O_3 has a rather poor solubility, while its oxidation product VO_4^{3-} is readily soluble in highly alkaline solutions. For Sb_2O_3, it is vice versa. As_2O_3 as well as As_2O_5 are well-soluble in the hydroflux medium. Therefore, As_2O_3 was mainly applied as reducing agent. The observed solubility of these oxides under hydroflux conditions is comparable to the one in diluted alkaline solutions.[24–26]

For the synthesis of K_2Te_3, the molar ratio $q(Te) = n(As_2O_3):n(TeO_2) = 1.2$ was used. After sealing the autoclave, the mixture was reacted for 48 hours at 200 °C, before it was cooled down to room temperature within 24 h. The reaction product consisted of large black bar-shaped crystals of K_2Te_3 (Figure 1) and a pale purple solution. Experiments with q(Te) of 1.0 or 0.75 also resulted in the crystallization of K_2Te_3. Despite the sub-stoichiometric content of the reducing agent

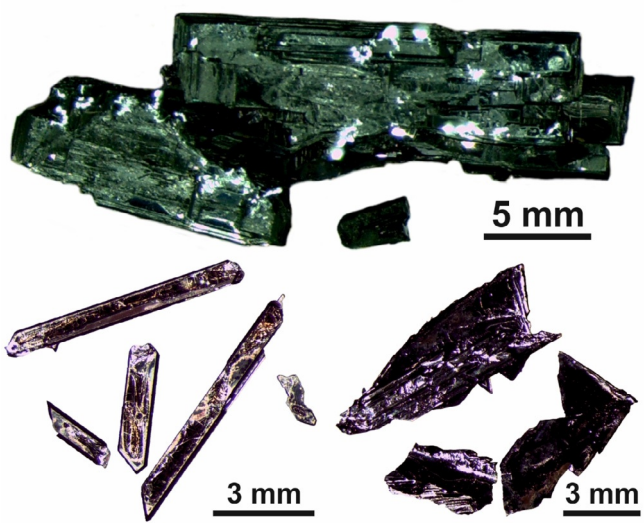

Figure 1. Selected crystals of K_2Te_3 (top), K_2Se_3 (bottom left) and K_2Se_2Te (bottom right) obtained from hydroflux syntheses.

in these experiments (for an equation see below), there was no evidence of the formation of elemental tellurium. In experiments with q(Te) ratios larger than 1.2, K_2Te_3 did not form.

Substantially shorter reaction times decreased the yield of K_2Te_3 while the purple color of the solution intensified. The purple solutions are sensitive against water and air, resulting in the precipitation of elemental tellurium. Spectroscopic analysis of this purple solution point towards the ditelluride ion Te_2^{2-} (see below).

The syntheses of selenides from SeO_2 under hydroflux conditions followed the same procedure. To synthesize K_2Se_3, the molar ratio $q(Se) = n(As_2O_3):n(SeO_2) = 1.2$ was used with a reactant concentration of about $c(SeO_2) = 1\,mol\,L^{-1}$. Hence, $c(SeO_2)$ was about ten times higher than $c(TeO_2)$ needed for the crystallization of K_2Te_3. The reaction product consisted of a deep red solution and large K_2Se_3 crystals (Figure 1). Experiments with lower reactant concentrations yielded only in a deep red solution without any solid product. The red solution contained diselenide anions Se_2^{2-} (see below).

By using a larger excess of reducing agent, the intense color of the dichalcogenide solutions vanished at $q(Ch) = 3.0$. Furthermore, when dissolved As_2O_3 is added to the colored dichalcogenide solutions at room temperature, colorless solutions are obtained. Both observations indicate the formation of monochalcogenide anions Ch^{2-}. Equation (4) summarizes the reduction of the dichalcogenide anions:

$$Ch_2^{2-} + AsO_3^{3-} + 2\,OH^- \rightarrow 2\,Ch^{2-} + AsO_4^{3-} + H_2O \quad (4)$$

A mixture containing TeO_2 and SeO_2 yielded neither a mixture of K_2Se_3 and K_2Te_3 nor a solid solution with the two anions in one solid, but K_2TeSe_2. The small difference in the electronegativity (Pauling: Se 2.5, Te 2.1) is sufficient to assign the two elements their roles according to the charge distribution in the heteroatomic Ch_3^{2-} anion. The increased intramolecular polarity in the diselenotellurate(II) $^-(Se^{-II}$–Te^{II}–$Se^{-II})^-$ compared to the triselenide $^-(Se^{-I}$–Se^{0}–$Se^{-I})^-$ is

symbolized, but certainly also overemphasized, by the oxidation states.

K_2TeSe_2 was synthesized under reaction conditions similar to those of the homoatomic trichalcogenides, using SeO_2 and TeO_2 in the molar ratio of 2:1. Adding an excess of about 5% of SeO_2 helped to avoid the co-crystallization of K_2Te_3, which is less soluble in the hydroflux than K_2Se_3. An amount of 1.3 equivalents of the reducing agent As_2O_3 was added (based on $^2/_3\,SeO_2 + {}^1/_3\,TeO_2$). Similar to the synthesis of K_2Se_3, relatively high reactant concentrations are necessary to obtain crystals of K_2TeSe_2.

It was surprising to obtain hygroscopic trichalcogenides from their dioxides in a hydroflux, which (a) contains water and (b) is usually stabilizing high oxidation states. In this case, the As_2O_3, which had initially been added for other reasons, acted as the reducing agent and was itself oxidized to arsenic(V). Arsenic is not only the electron donor but binds the oxygen atoms provided by the chalcogen(IV) oxides in AsO_4^{3-} anions. This redox chemistry is far from what the standard potentials let expect, but can be rationalized by Equation (5):

$$7\,As_2O_3 + 6\,ChO_2 + 4\,K^+ + 46\,OH^- \rightarrow 2\,K_2Ch_3 + 14\,AsO_4^{3-} + 23\,H_2O \quad (5)$$

The redox reaction is promoted by the high concentration of hydroxide ions on the side of the reactants. Moreover, the hydroflux is highly hygroscopic. The initially contained water but also water formed through the reaction are strongly bonded to hydroxide ions. Thereby, the activity of the water is considerably reduced, which does not only decrease its vapor pressure and drives the reaction but obviously prevents the hydrolysis of the water sensitive trichalcogenides. On the other hand, the reaction diluted the hydroflux so that it did not solidify upon cooling to room temperature. Washing of the reaction product with a protic solvent, for example, an alcohol, strongly increases the activity of water and thereby induces the decomposition of K_2Ch_3. Similar observations had been made for other water sensitive products from hydroflux syntheses, for example, $K_2[Fe_2O_3(OH)_2]$ or Tl_3IO.[27,28] Also several aprotic polar solvents, for example, DMF, proved to be unsuitable for rinsing because potassium hydroxide is less soluble in them than the trichalcogenides. Therefore, the products were filtered under inert conditions by using a Schlenk-frit. The yields with respect to the used ChO_2 were 90% for K_2Te_3, 60% for K_2Se_3 and 80% for K_2Se_2Te, related to the solubility of the diverse chalcogenide species. The adhering KOH together with the genuine moisture-sensitivity of K_2Ch_3 necessitated storage and handling of the crystals under inert conditions (argon). The powder X-ray diffraction patterns of the isolated crystals showed single-phase products, but small residuals of the hydroflux were visible in the scanning electron microscope (Figure S1 to S4, Table S1, Supporting Information).

X-ray diffraction on black single-crystals of K_2Se_3 ($Cmc2_1$) and K_2Te_3 ($Pnma$) confirmed the known structures.[4,5] For the new compound K_2TeSe_2 an orthorhombic structure in the non-centrosymmetric space group $Cmc2_1$ (no. 36) was found with the lattice parameter $a = 783.42(4)$ pm, $b = 1045.64(6)$ pm, and $c = 777.13(4)$ pm at 100(1) K. Details on the structure determinations and the atomic parameters of the three compounds can be found in Tables S2 to S8, Supporting Information. Selected bond lengths and angles are listed in Table S9, Supporting Information.

K_2TeSe_2 is isostructural to K_2Se_3 and K_2S_3 (Figure 2). The angulate diselenotellurate(II) anion, $(TeSe_2)^{2-}$, has crystallographic C_{2v} symmetry with two equal Se–Te bond lengths of 256.2(1) pm and a Se–Te–Se angle of 97.6(1)°. The $(TeSe_2)^{2-}$ anion had previously been found in $(2,2,2\text{-crypt-K})_2(TeSe_2)\cdot en$ (en = ethylendiamin)[29] and $[Mn(en)_3](TeSe_2)$[30] with Te–Se bond lengths of about 250 pm and 250.3(1) pm as well as Se–Te–Se angles of 111.3(1)° and 102.6(1)°, respectively. In these structures, the $(TeSe_2)^{2-}$ anions are well separated from each other and interact with hydrogen atoms of the organic ligands. The wider Se–Te–Se angles are consistent with the shorter Te–Se bond lengths, which increase the repulsion between the terminal atoms. In K_2TeSe_2, short intermolecular distances of 333.4(1) pm suggest secondary bonds $Te^{II}\cdots Se^{-II}$, which, together with stronger cation-anion interactions, might be responsible for the elongated primary Te–Se bond. In alkali metal trichalcogenides A_2Ch_3 (A = K–Cs; Ch = S–Te) with homonuclear anions, which have a lower intramolecular polarity than $(TeSe_2)^{2-}$, the shortest intermolecular distances range from 344 pm to 386 pm.[31]

Besides K_2TeSe_2, the following compounds crystallize in the K_2S_3 structure type: A_2Ch_3 (A = K–Cs; Ch = S, Se), Cs_2Te_3 and Cs_2TeS_2.[4,31–33] The bond angle in the Ch_3^{2-} anions deceases from the sulfides (average angle of 106.0°) via the selenides (average angle of 103.1°) to the telluride (100.1° in Cs_2Te_3).[31] This can be attributed to a decreasing s-orbital contribution to the bonding when proceeding to the heavier main-group elements. Despite its smaller terminal atoms, the anion in Cs_2TeS_2 has a slightly wider bond angle (99.4°) than $(TeSe_2)^{2-}$ in K_2TeSe_2, which might be an effect of the higher electronegativity and thus the higher partial charge of the sulfur atoms compared to selenium.

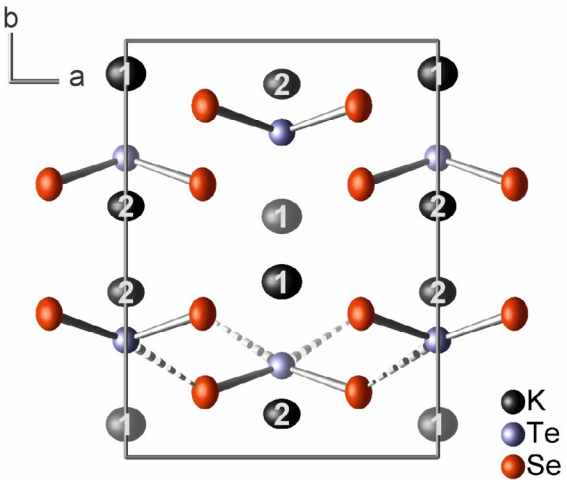

Figure 2. Crystal structure of K_2TeSe_2 projected along the [001] direction. The secondary bonds $Te^{II}\cdots Se^{-II}$ are dotted. Ellipsoids enclose 99.99% of the probability density of the atoms at 100(1) K.[58]

In the crystal structure of K_2TeSe_2, the $(TeSe_2)^{2-}$ anions form double-layers parallel to (010) (Figure 2) with the tellurium atoms pointing towards the inside of the double layer. The potassium atoms separate the double layers. The polarity of the structure is evident, as all $(TeSe_2)^{2-}$ "arrowheads" point into the same direction along [001] (Figure S5, Supporting Information). The two potassium atoms K1 and K2 are each coordinated by six selenium atoms in the shape of distorted trigonal prisms with C_s symmetry (Figure 3). Within those polyhedra, the K–Se bond lengths range from 338.9(1) pm to 360.9(1) pm and from 338.3(1) pm to 349.6-

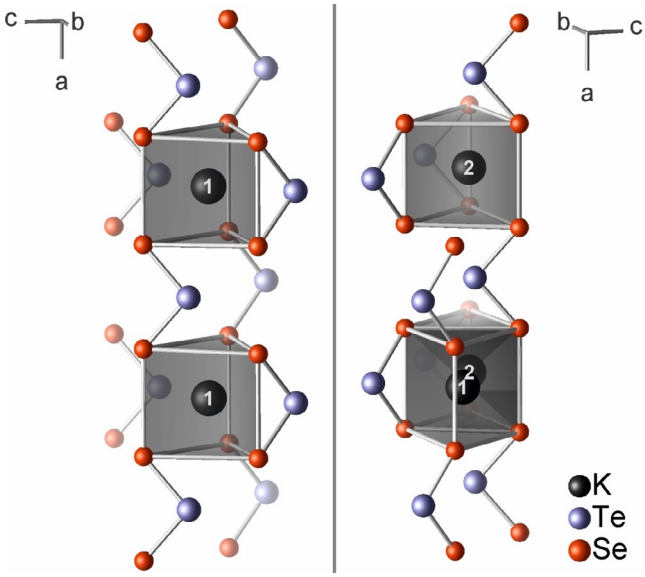

Figure 3. Two views of the coordination polyhedra of the potassium cations in K_2TeSe_2. The two potassium atoms share the uncapped square face of their trigonal prism.

(1) pm, respectively (Table S8, Supporting Information). The slightly larger polyhedron around K1 involves six $(TeSe_2)^{2-}$ anions, whereas only five anions form the trigonal prism around K2. Comparing the $[KSe_6]$ polyhedra of K_2Se_3 and K_2TeSe_2, the sum of their volumes is about 5% larger for the latter. The $[KSe_6]$ prisms of K1 and K2 share the square face that is not capped by a tellurium atom (K···Te 340.8(1) to 390.7(1) pm). The $[K_2Se_8]$ double prisms share corners and edges to form a three-dimensional framework. In K_2TeSe_2, the shortest K···K distance is with 366.7(1) pm even shorter than in K_2Se_3 [369.4(1) pm], but not as short as in K_2S_3 [359.2(2) pm].[4] In K_2Te_3, which crystallizes in its own structure type, the shortest distance between cations is 441.0(1) pm.

To obtain further insight into the chemical processes in the hydroflux, especially the prevalent chalcogenide anions Ch_n^{2-} ($n = 1, 2, 3$), the reacted solutions were analyzed by UV/Vis and Raman spectroscopy. The reaction conditions were $q(K) = 1.9$ and 200 °C, as for the above syntheses, but the reaction time was only five hours. The reactant concentration of the syntheses for the UV/Vis measurements was about 0.01 mol L^{-1}, while the concentration for the Raman measurements was about 30 times higher. Analyses were performed under ambient conditions in air and at room temperature. During the UV/Vis measurements, the lower limit in wavelength was about 240 nm because of strong absorption by the hydroflux medium. Raman and UV-vis spectra of each single reactant dissolved in a hydroflux with $q(K) = 1.9$ can be found in Figure S6 to S11, Supporting Information.

Purple solutions were obtained starting from a molar ratio of As_2O_3 and TeO_2 of $q(Te) = 1$. In this ratio, the complete oxidation of arsenic(III) to arsenic(V) provides four electrons per tellurium(IV) atom. The UV/Vis spectrum of such a sample show an absorption band with a maximum at 522 nm (Figure 4), which is slightly shifted to lower frequencies in comparison with the published values for ditelluride anions Te_2^{2-} of 508 to 512 nm.[34–37] In diluted alkaline solutions, the presence of the purple Te_2^{2-} had been observed and analyzed in various experimental setups, e.g., as a product of accidental oxidation of monotelluride solutions by oxygen from leakage,[34,35] after the oxidation of monotelluride solution in a photochemical cell by irradiation of CdTe,[35] in an electrolysis starting from a monotelluride solution[35] or during an electrolysis generating monotelluride that further reacted with elemental tellurium to form the ditelluride anion.[36,37] Moreover, the absorption spectrum of the isoelectronic iodine molecule I_2 dissolved in hexane exhibits a similar band with a maximum at about 520 nm.[34,38]

The Raman spectra of experiments with $q(Te) = 0.75, 1$, or 1.5 (i.e. 3, 4, 6 electrons per Te^{IV}) show a vibration band at 181 cm^{-1} (Figure 4), which occurs in an energy range typical

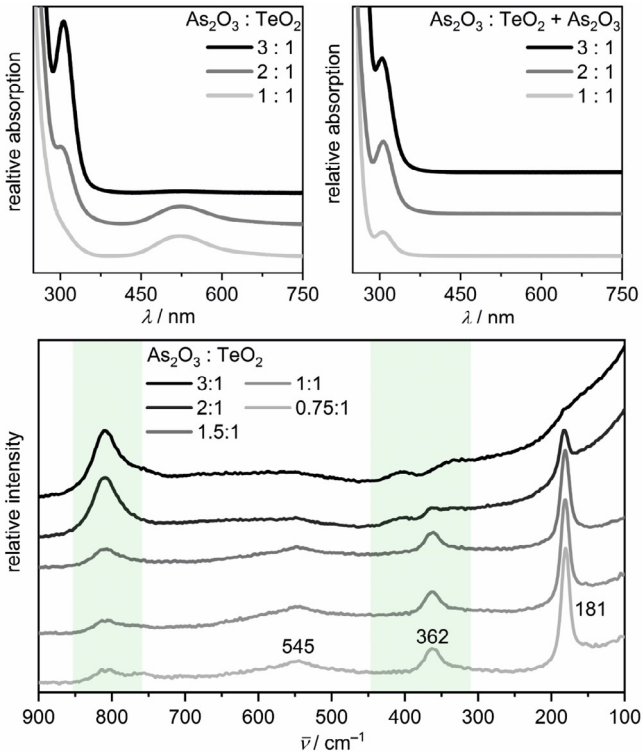

Figure 4. UV/Vis (top left) and Raman (bottom) spectra of telluride solutions synthesized with different q(Te) ratios. Absorption spectra of telluride solutions after adding dissolved As_2O_3 at room temperature are presented (top right). The green boxes mark the wavenumber range, where As–O vibrations of the AsO_4^{3-} anion occur.

for oligotellurides.[17,39–41] We found no literature data for Te–Te vibrations of tellurides in aqueous solutions. K_2Te_2 dissolved in DMF shows a vibration at 164 cm^{-1}.[17] The Raman vibrations of the pentatelluride ion Te_5^{2-} in acetone are located at 170 cm^{-1} and 195 cm^{-1}.[39] The Te–Te bands in As–Te and Se–Te glasses were reported to occur at 155 cm^{-1} and 175 cm^{-1}.[40,41] Consequently, and as indicated by the UV/Vis spectra, we assign the band at 181 cm^{-1} to the vibration of the Te_2^{2-} anion. The bands observed at 362 cm^{-1} and 545 cm^{-1} represent the first and second overtone of the 181 cm^{-1} vibration band, respectively. The presence of these overtones and the high intensity of the Te–Te vibration band compared to the spectra of the selenides are caused by Raman resonance of the 532 nm laser with the absorption band at 522 nm.

When the amount of reducing agent is increased, the purple color of the solution fades until a colorless solution is obtained in syntheses starting from $q(\mathrm{Te}) = 3$ (i.e. 12 electrons per Te^{IV}). These solutions as well as samples for which dissolved As_2O_3 was added at room temperature to purple Te_2^{2-} solutions showed a single symmetrical absorption band in the UV/Vis with a maximum at 324 nm (Figure 4). This is in good agreement with the published value of 325 nm for Te^{2-} in diluted alkaline solutions.[34,36] In the corresponding Raman spectra, no band was detectable in the typical energy range of Te–Te vibrations, as can be expected for the monotelluride anion Te^{2-} being the predominant species. The protonated monotelluride HTe^- (270 nm)[34] was not observed in our experiments. This can be expected for ultra-alkaline media, as the second acid dissociation constant pK_{a2} of hydrogen telluride H_2Te had been reported to be 12.2.[42]

In none of the solutions, the tritelluride anion Te_3^{2-} could be detected spectroscopically. It had been reported to have an UV/Vis absorption band at 376 nm in DMF,[18] and K_2Te_3 dissolved in liquid ammonia or DMF exhibits a vibration band at about 162 cm^{-1}.[17] In the hydroflux medium, the slow crystallization of K_2Te_3 during the synthesis at 200 °C and its insolubility at room temperature suggest an equilibrium between the telluride species similar to Equation (1), in which the tritelluride anion is non-preferential. The precipitation of K_2Te_3 is thus not caused by a high concentration of Te_3^{2-} but a very small solubility product. These observation are in line with reported electrochemical experiments on the reductive dissolution of a tellurium cathode: while at pH 9 mainly Te^{2-} anions formed, Te_2^{2-} anions dominated above pH 12.[43]

In low-concentrated alkaline solutions, the optical absorption band of the diselenide anion Se_2^{2-} had been reported at about 430 nm.[19,20,23] Se_3^{2-} and Se_4^{2-} absorb at 530 nm and 470 nm, respectively.[19] The UV/Vis spectrum (Figure 5) of an orange solution synthesized with $q(\mathrm{Se}) = 1$ in hydroflux exhibited a symmetrical absorption band with its maximum at 440 nm, which we attribute to Se_2^{2-} with respect to the above cited literature. For higher q(Se) ratios, viz. 2 and 3, the formation of the monochalcogenide anion was observed in the UV/Vis, similar as in the case of the tellurides.

Raman spectra of dissolved oligoselenides are scarce. In acetone, the Se_6^{2-} anion exhibits vibrations bands at 235 cm^{-1}, 285 cm^{-1} and 405 cm^{-1}.[39] In low-concentrated alkaline solutions, the oxidation of H_2Se with H_2O_2 had yielded selenium species with average oxidations states of −1, −0.67 and −0.5, that is, Se_n^{2-} ($n = 2, 3, 4$), and Raman bands at 269 cm^{-1} and 324 cm^{-1}.[22] The band at 269 cm^{-1} had been assigned to the Se_4^{2-} anion based on the Raman resonance of a measurement with a 476 nm laser,[22] since the Se_4^{2-} anion has an absorption band at 470 nm.[19] A Raman spectrum measured with an 457 nm laser had resulted in an even greater intensity of the 269 cm^{-1} band.[22] DFT calculations had predicted two Raman active vibration modes at 299 cm^{-1} and 106 cm^{-1} for the Se_4^{2-} anion and one Raman band at 273 cm^{-1} for Se_2^{2-}.[22] In glassy selenium, the Se–Se stretching mode had been reported to occur at 250 cm^{-1} with a shoulder at 235 cm^{-1},[44] which is similar to As–Se (238 cm^{-1}, 252 cm^{-1})[45] and Se–Te glasses (220 cm^{-1} to 280 cm^{-1}).[41]

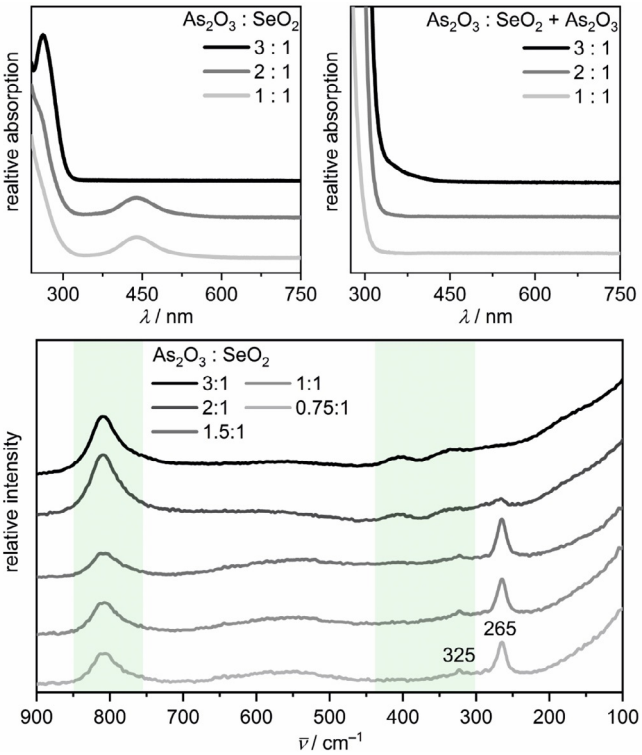

Figure 5. UV/Vis (top left) and Raman (bottom) spectra of selenide solutions synthesized with different q(Se) ratios. Absorption spectra of selenide solutions after adding dissolved As_2O_3 at room temperature are presented (top right). The green boxes mark the wavenumber range, where As–O vibrations of the AsO_4^{3-} anion occur.

The Raman spectra (Figure 5) of solutions obtained from hydroflux reactions with q(Se) of 0.75, 1, or 1.5 show a vibration band with a maximum at 265 cm^{-1}, which could indicate higher oligoselenides, although the transmission UV/Vis spectra revealed exclusively Se_2^{2-} for $q(\mathrm{Se}) = 1$. However, the concentration in the optical spectroscopy had to be about 30 times lower than for the Raman measurements when using standard quartz cuvettes. To exclude a concentration dependent product formation, we measured an UV/Vis spectrum in reflection mode on the same selenide solution used in the Raman spectroscopy, which showed only one absorption band at 435 nm confirming the presence of mainly Se_2^{2-} anions (Figure S12, Supporting Information). Therefore and because

of the absence of additional vibration bands[22] we assign the 265 cm^{-1} band in the Raman spectra of the experiments with $q(Se) = 0.75$, 1, or 1.5 to the diselenide anion Se_2^{2-}, which is also in good agreement with the calculated value of 273 cm^{-1}.[22]

In all of our experiments, the diselenide band at 265 cm^{-1} was accompanied by a tiny band at 323 cm^{-1}, which was proposed to be caused by Se_2^-.[22] Both vibration bands had always the same intensity ratio, despite different $q(Se)$. It had been stated that the Se_2^- radical forms under intense laser light from oligoselenides Se_n^{2-} with $n = 2$–4.[19,22] However, Se_2^{2-} is an unlikely precursor, as an electron would have to be abstracted. Moreover, the excitation of Se_2^{2-} with a 530 nm laser would be very inefficient because of its absorption band at 440 nm. The most plausible precursor for Se_2^- is Se_4^{2-}, since its decomposition involves a symmetrical bond cleavage and its absorption band at 470 nm is close to the wavelength of the laser.[19,22] The dissociation of Se_3^{2-} would result in the Se^- radical besides Se_2^-, which had been observed in aqueous solutions.[46] In our experiments, the presence of small amounts of other oligoselenides than Se_2^{2-} can be explained by Equation (2) and (3). In addition, the Se_2^- radical is known to have an absorption band between 490 and 520 nm[47–49] leading to an intensity enhancement of its vibration band at 323 cm^{-1} by Raman resonance, so that the actual Se_2^- radical concentration is expectedly low. When changing the radiation source to a 1064 nm laser, the vibrations band at 323 cm^{-1} vanishes, while the Se_2^{2-} band remains with no change in intensity (Figure S13, Supporting Information).

In the UV/Vis spectrum of the experiment with $q(Se) = 3$ (Figure 5), the monoselenide anion Se^{2-} exhibits one absorption band at 262 nm, which is close to the reported value of 270 nm.[19,20] The same result was obtained for a solution with higher concentration of the reactants, which were used for Raman spectroscopy (Figure S14, Supporting Information). The Raman spectra confirmed the absence of species with Se–Se bond.

By adding at room temperature a hydroflux solution of As_2O_3 with the same $q(K)$ to an orange-colored diselenide solution with $q(Se) = 1$, the color and the absorption band of the Se_2^{2-} anion vanishes. In this case, the strong absorption of the excess AsO_3^{3-} ions below 300 nm overlays the signal of the monoselenide anion Se^{2-} (Figure S6, Supporting Information).

As the vibration bands of AsO_4^{3-} and SeO_3^{2-} overlap, we also used Sb_2O_3 as reducing agent. The reacted solution with $n(Sb_2O_3):n(SeO_2) = 0.75$ showed the Raman band of Se_2^{2-} at 265 cm^{-1} (Figure S15, Supporting Information). The additional vibrational band at 810 cm^{-1} is in good agreement with the Raman spectrum of SeO_2 dissolved under hydroflux conditions. The coexistence of SeO_3^{2-} and Se_2^{2-} anions confirmed the observation that no elemental selenium was formed in our experiments.

The heterochalcogenide solutions were prepared by starting from SeO_2 and TeO_2 in the molar ratio 2:1, according to the molar fractions of the chalcogens in K_2Se_2Te. As_2O_3 was added as reducing agent in 1, 1.5 and 2 equivalents, i.e., $q(SeTe) = As_2O_3:(^2/_3 SeO_2 + {}^1/_3 TeO_2)$. The UV/Vis spectrum of the experiment with $q(SeTe) = 1$ shows the Se_2^{2-} band at

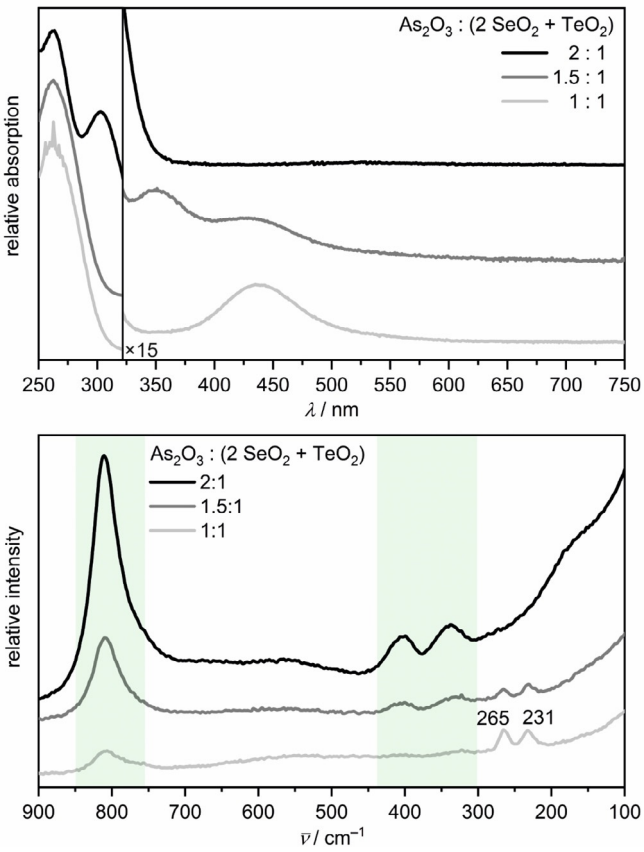

Figure 6. UV/Vis (top) and Raman (bottom) spectra of chalcogenide solutions synthesized with different q(SeTe) ratios. The green boxes mark the wavenumber range, where As–O vibrations of the AsO_4^{3-} anion occur.

435 nm as well as the Se^{2-} band at 262 nm (Figure 6), while in the spectrum for $q(SeTe) = 1.5$, one additional band appears at 351 nm. There is very little spectroscopic information on mixed chalcogenides that could be used for comparison. NMR experiments on the mixed chalcogenides $(TeSe_2)^{2-}$ and $(TeSe_3)^{2-}$ in ethylenediamine revealed several equilibria between those anions and tellurium richer phases, for example, $(Te_2Se)^{2-}$ and $(Te_3Se)^{2-}$.[50] In analogy, we propose a similar equilibrium between the diselenide and ditelluride anions [Eq. (6)]. Consequently, the absorption band at 351 nm is assigned to the $(SeTe)^{2-}$ anion, which was not described before.

$$Se_2^{2-} + Te_2^{2-} \rightleftharpoons 2\,(SeTe)^{2-} \qquad (6)$$

The Raman spectra (Figure 6) for $q(SeTe) = 1$ and 1.5 show the Se_2^{2-} band at 265 cm^{-1} and one additional band at 231 cm^{-1}, which occurs in the typical energy range of Se–Te vibrations and is therefore assigned to the $(SeTe)^{2-}$ anion.[41,51–54] The Se–Te stretching vibrations in Se–Te glasses had been reported to occur between 205 cm^{-1} and 216 cm^{-1}.[52,53] A similar shift to lower energies had been observed for Se–Se and Te–Te vibrations in the solid state compared with Se_2^{2-} and Te_2^{2-} anions in aqueous solutions. DFT calculations on mixed trichalcogenides Ch_3^{2-} (Ch = Se,

Te) had predicted a range from 218 cm^{-1} to 230 cm^{-1} for Se–Te stretching modes.[41] In $[Zn(NH_3)_4](TeSe_3)$, they occur at 217 cm^{-1} and 231 cm^{-1},[54] in Na_2TeSe_3 at 213 cm^{-1} and 238 cm^{-1}.[51]

The vibrations bands of the Se_2^{2-} and the $(SeTe)^{2-}$ anions are clearly detectable. The Se_2^{2-} band is the more intense for $q(SeTe) = 1$, but the weaker for $q(SeTe) = 1.5$. As indicated by the Raman spectra, TeO_2 is only partly reduced, as small intensities of Te–O vibrations of the TeO_3^{2-} anion are visible with $q(SeTe) = 1$ (Figure S16, Supporting Information). The assumption of $(SeTe)^{2-}$ anions that formed from a 2:1 solution of SeO_2 and TeO_2 is indirectly corroborated by the remaining Se_2^{2-}anions visible in the Raman spectrum. The Raman spectrum of the experiment with $q(SeTe) = 1.5$ has an overall lower intensity of the chalcogenide vibration bands than the one with $q(SeTe) = 1$, since the crystallization of K_2Se_2Te has lowered the concentration of dissolved chalcogenide anions.

The UV/Vis spectrum of the experiment with $q(SeTe) = 2$ shows the absorption bands of Se^{2-} at 261 nm and Te^{2-} at 305 nm, indicating that the high amount of As_2O_3 had reduced the chalcogenide(IV) oxides completely. Accordingly, no Raman band is found in the range of *Ch*–*Ch* vibrations.

When mixing pre-synthesized Se_2^{2-} and Te_2^{2-} solutions at room temperature, the resulting mixture shows a strong $(SeTe)^{2-}$ band at 231 cm^{-1} and a smaller Se_2^{2-} band at 265 cm^{-1} (Figure S17, Supporting Information). The crystallization of K_2Te_3 had reduced the Te_2^{2-} concentration, while the concentration was too low for the precipitation of K_2Se_3. This experiment corroborates the equilibrium in Equation (6).

The chalcogenide solutions were sensitive against atmosphere. The colorless monotelluride solutions started to oxidize on the slightest contact with oxygen resulting in purple solutions containing Te_2^{2-}, from which then elemental tellurium precipitated. The latter can be identified by Te–Te vibration bands at 120 cm^{-1} and 139 cm^{-1} (Figure S18, Supporting Information).[55] The reaction takes place on the surface of the liquid, which allows handling them in air for a short period. Upon adding As_2O_3 solution, the tellurium is again reduced to tellurides (Figure S19, Supporting Information).

The selenide solutions are less reactive. Monoselenide solutions showed the orange color of Se_2^{2-} only after several hours in air. When diselenide solutions were diluted with water and exposed to air, a red film initially formed on the surface of the liquid, which yielded a grey powder after several hours that showed Se-Se vibrations bands at 140 cm^{-1} and 235 cm^{-1} (Figure S18, Supporting Information).[56,57] Higher oligochalcogenides could not be detected.

Experiments concerning the reductive potential of As and As_2O_3 yielded unexpected results, e.g., that elemental arsenic is unable to reduce Ch_2^{2-} to Ch^{2-}, and that excess $As^{III}O_3^{3-}$ anions seem to disproportionate into arsenic and $As^{V}O_4^{3-}$ (see Supporting Information).

Conclusion

Solutions of mono- and dichalcogenide anions Ch^{2-}, Ch_2^{2-} (Ch = Se, Te) and $(SeTe)^{2-}$ are accessible by reducing the respective ChO_2 with As_2O_3 under hydroflux conditions. When a sub-stoichiometric amount of As_2O_3 is added, the reaction product consists of a mixture of ChO_3^{2-} and Ch_2^{2-} anions. However, neither elemental chalcogen nor oligochalcogenide anions larger than Ch_2^{2-} were observed spectroscopically. The addition of As_2O_3 in excess yields colorless solutions of monochalcogenide anions Ch^{2-}. Large single-crystals of K_2Ch_3 were obtained when the amount of As_2O_3 does not allow an average oxidation state of the chalcogen that is more negative than −0.67 (Ch_3^{2-}). The crystallization of K_2Se_3 or K_2Se_2Te requires higher reactants concentrations than needed for K_2Te_3.

The preparation of chalcogenides via the hydroflux method represents an attractive alternative to the hitherto used synthesis routes. The necessary equipment is cheaper and the procedure is simpler and also safer. The unexpected formation of chalcogenides from chalcogen dioxides is due to the ultra-alkaline conditions. The water in the reaction mixture is strongly bonded to hydroxide. Its reduced activity prevents the hydrolysis of the trichalcogenides, but also shifts the redox equilibria known from dilute alkaline solutions.[24] A transfer of the approach to other systems should be possible.

Acknowledgements

We thank Prof. Dr. E. Brunner, TU Dresden, for the opportunity to use the Raman- and UV/Vis spectrometers. This work was financially supported by the Deutsche Forschungsgemeinschaft (DFG, project-id 438795198). Open access funding enabled and organized by Projekt DEAL.

Conflict of Interest

The authors declare no conflict of interest.

Keywords: crystal structure · hydroflux · selenium · spectroscopy · tellurium

[1] E. Zintl, J. Goubean, W. Dullenkopf, *Z. Phys. Chem.* **1931**, *154A*, 1–46.
[2] E. Zintl, A. Harder, B. Dauth, *Z. Elektrochem.* **1934**, *40*, 588–593.
[3] W. Klemm, H. Sodomann, P. Langmesser, *Z. Anorg. Allg. Chem.* **1939**, *241*, 281–304.
[4] P. Böttcher, *Z. Anorg. Allg. Chem.* **1977**, *432*, 167–172.
[5] B. Eisenmann, H. Schäfer, *Angew. Chem. Int. Ed. Engl.* **1978**, *17*, 684–684; *Angew. Chem.* **1978**, *90*, 731–731.
[6] P. Böttcher, J. Getzschmann, R. Keller, *Z. Anorg. Allg. Chem.* **1993**, *619*, 476–488.
[7] I. Schewe, P. Böttcher, *Z. Naturforsch. B* **1990**, *45*, 417–422.
[8] I. Schewe-Miller, P. Böttcher, *Z. Kristallogr. - Cryst. Mater.* **1991**, *196*, 137–151.

[9] R. Zagler, B. Eisenmann, *Z. Kristallogr. - Cryst. Mater.* **1988**, *183*, 193 – 200.
[10] G. Thiele, L. Vondung, S. Dehnen, *Z. Kristallogr. - Cryst. Mater.* **2016**, *231*, 257 – 260.
[11] W. M. Chance, D. E. Bugaris, A. S. Sefat, H.-C. zur Loye, *Inorg. Chem.* **2013**, *52*, 11723 – 11733.
[12] R. Albrecht, J. Hunger, M. Hoelzel, E. Suard, W. Schnelle, T. Doert, M. Ruck, *Eur. J. Inorg. Chem.* **2021**, 364 – 376.
[13] R. Albrecht, J. Hunger, T. Doert, M. Ruck, *Eur. J. Inorg. Chem.* **2019**, 1398 – 1405.
[14] K. D. zur Loye, W. M. Chance, J. Yeon, H.-C. zur Loye, *Solid State Sci.* **2014**, *37*, 86 – 90.
[15] R. Albrecht, J. Hunger, T. Doert, M. Ruck, *Z. Anorg. Allg. Chem.* **2020**, *646*, 1130 – 1137.
[16] L. D. Schultz, *Inorg. Chim. Acta* **1990**, *176*, 271 – 275.
[17] L. D. Schultz, E. T. Davis, J. D. Lewis, *Spectrosc. Lett.* **2013**, *46*, 191 – 194.
[18] J. L. McAfee, J. R. Andreatta, R. S. Sevcik, L. D. Schultz, *J. Mol. Struct.* **2012**, *1022*, 68 – 71.
[19] L. E. Lyons, T. L. Young, *Aust. J. Chem.* **1986**, *39*, 511 – 527.
[20] S. Licht, F. Forouzan, *J. Electrochem. Soc.* **1995**, *142*, 1546 – 1551.
[21] C. C. Raymond, D. L. Dick, P. K. Dorhout, *Inorg. Chem.* **1997**, *36*, 2678 – 2681.
[22] A. Goldbach, J. Johnson, D. Meisel, L. A. Curtiss, M.-L. Saboungi, *J. Am. Chem. Soc.* **1999**, *121*, 4461 – 4467.
[23] A. Goldbach, M.-L. Saboungi, J. A. Johnson, A. R. Cook, D. Meisel, *J. Phys. Chem. A* **2000**, *104*, 4011 – 4016.
[24] A. F. Holleman, E. Wiberg, N. Wiberg, *Lehrbuch Der Anorganischen Chemie*, Walter De Gruyter & Co., Berlin, Germany, **2007**.
[25] T. Y. Karlsson, *Studies on the Recovery of Secondary Antimony Compounds from Waste*, PhD Thesis, Chalmers University Of Technology, Gothenburg, Sweden, **2017**.
[26] X. Hu, Y. Yue, X. Peng, *J. Environ. Sci.* **2018**, *67*, 96 – 103.
[27] R. Albrecht, J. Hunger, M. Hölzel, T. Block, R. Pöttgen, T. Doert, M. Ruck, *ChemistryOpen* **2019**, *8*, 1399 – 1406.
[28] R. Albrecht, H. Menning, T. Doert, M. Ruck, *Acta Crystallogr. Sect. E* **2020**, *76*, 1638 – 1640.
[29] M. Bjorgvinsson, J. F. Sawyer, G. J. Schrobilgen, *Inorg. Chem.* **1991**, *30*, 4238 – 4245.
[30] F. Wendland, C. Näther, W. Bensch, *Z. Naturforsch. B* **2000**, *55*, 871 – 876.
[31] P. Böttcher, *J. Less-Common Met.* **1980**, *70*, 263 – 271.
[32] P. Böttcher, *Z. Anorg. Allg. Chem.* **1980**, *461*, 13 – 21.
[33] J.-M. Babo, K. K. Wolff, T. Schleid, *Z. Anorg. Allg. Chem.* **2013**, *639*, 2875 – 2881.
[34] R. J. Myers, *J. Solution Chem.* **2007**, *36*, 395 – 403.
[35] A. B. Ellis, S. W. Kaiser, J. M. Bolts, M. S. Wrighton, *J. Am. Chem. Soc.* **1977**, *99*, 2839 – 2848.
[36] S. G. B. Passos, D. V. Freitas, J. M. M. Dias, E. T. Neto, M. Navarro, *Electrochim. Acta* **2016**, *190*, 689 – 694.
[37] R. T. Ribeiro, J. M. M. Dias, G. A. Pereira, D. V. Freitas, M. Monteiro, P. E. C. Filho, R. A. Raele, A. Fontes, M. Navarro, B. S. Santos, *Green Chem.* **2013**, *15*, 1061 – 1066.
[38] R. J. Chance, M. Shaw, L. Telgmann, M. Baxter, L. J. Carpenter, *Atmos. Meas. Tech.* **2010**, *3*, 177 – 185.
[39] R. G. Teller, L. J. Krause, R. C. Haushalter, *Inorg. Chem.* **1983**, *22*, 1809 – 1812.
[40] A. Tverjanovich, K. Rodionov, E. Bychkov, *J. Solid State Chem.* **2012**, *190*, 271 – 276.
[41] A. Tverjanovich, A. Cuisset, D. Fontanari, E. Bychkov, *J. Am. Chem. Soc.* **2018**, *101*, 5188 – 5197.
[42] A. J. Panson, *J. Phys. Chem.* **1963**, *67*, 2177 – 2180.
[43] A. J. Panson, *J. Phys. Chem.* **1964**, *68*, 1721 – 1724.
[44] G. Carini, M. Cutroni, G. Galli, P. Migliardo, F. Wanderlingh, *Solid State Commun.* **1980**, *33*, 1139 – 1141.
[45] V. Kovanda, M. Vlček, H. Jain, *J. Non-Cryst. Solids* **2003**, *326 – 327*, 88 – 92.
[46] M. Schöneshöfer, W. Karmann, A. Henglein, *Int. J. Radiat. Phys. Chem.* **1969**, *1*, 407 – 423.
[47] R. J. H. Clark, T. J. Dines, M. Kurmoo, *Inorg. Chem.* **1983**, *22*, 2766 – 2772.
[48] H. Murata, T. Kishigami, R. Kato, *J. Phys. Soc. Jpn.* **1990**, *59*, 506 – 515.
[49] A. Goldbach, M. Grimsditch, L. Iton, M.-L. Saboungi, *J. Phys. Chem. B* **1997**, *101*, 330 – 334.
[50] M. Bjoergvinsson, G. J. Schrobilgen, *Inorg. Chem.* **1991**, *30*, 2540 – 2547.
[51] C. Pompe, C. Preitschaft, R. Weihrich, A. Pfitzner, *Inorg. Chem.* **2015**, *54*, 11457 – 11464.
[52] A. T. Ward, *J. Phys. Chem.* **1970**, *74*, 4110 – 4115.
[53] G. Delaizir, M. Dussauze, V. Nazabal, P. Lecante, M. Dollé, P. Rozier, E. I. Kamitsos, P. Jovari, B. Bureau, *J. Alloys Compd.* **2011**, *509*, 831 – 836.
[54] O. Kysliak, J. Beck, *Eur. J. Inorg. Chem.* **2013**, 124 – 133.
[55] J. U. Salmón-Gamboa, A. H. Barajas-Aguilar, L. I. Ruiz-Ortega, A. M. Garay-Tapia, S. J. Jiménez-Sandoval, *Sci. Rep.* **2018**, *8*, 8093.
[56] A. Puranen, M. Jansson, M. Jonsson, *J. Contam. Hydrol.* **2010**, *116*, 16 – 23.
[57] O. Kysliak, J. Beck, *J. Solid State Chem.* **2013**, *203*, 120 – 127.
[58] Deposition Numbers 2084650 (for K_2Se_3), 2084651 (for K_2Te_3) and 2084652 (for $K_2Se_2Te_2$) contain the supplementary crystallographic data for this paper. These data are provided free of charge by the joint Cambridge Crystallographic Data Centre and Fachinformationszentrum Karlsruhe Access Structures service www.ccdc.cam.ac.uk/structures.

Manuscript received: June 8, 2021
Accepted manuscript online: August 10, 2021
Version of record online: September 6, 2021

